

# Optimal Selection of Chromium and Titanium in Iron Alloy Based Coating Materials Deposited via HVOF

Ratnesh Kumar Sharma<sup>1</sup>, Shiv Ranjan Kumar<sup>2,\*</sup>, Anand Prakash<sup>3</sup>,  
Ajay Sharma<sup>4</sup>

<sup>1</sup>Mechanical engineering Department, Poornima College of Engineering, India

<sup>2</sup>Mechanical Engineering Department, Bhagalpur College of Engineering, Bhagalpur, India

<sup>3</sup>Mechanical Engineering Department, Supaul College of Engineering, Supaul, India

<sup>4</sup>Mechanical and Automation Engineering, Amity University, Noida, India

\*Author to whom correspondence should be addressed:

E-mail: ranjan.shiv@gmail.com

(Received December 03, 2024; Revised July 06, 2025; Accepted July 26, 2025)

**Abstract:** The goal of this work was to optimise the composition of the Fe-Cr-Ti alloy HVOF coating, taking into account both erosion resistance and mechanical characteristics. Using a special method that combined the fuzzy analytic hierarchy process (FAHP) and the technique for order preference by similarity to ideal solution (TOPSIS), the optimal formulation of the Fe-Cr-Ti alloy HVOF coating materials was found. The erosion properties include erosion wear rate under the condition of varying impact velocity and impingement angle. Fe-Cr-Ti alloy HVOF coating (C6) with 10% chromium and 10% titanium weight had the highest TOPSIS score of 0.748. Titanium is more significant than chromium regarding mechanical and wear behavior when considering all performance factors for the alloying element at levels up to 10%.

**Keywords:** chromium; Fe alloy-based coating; titanium; TOPSIS

## 1. Introduction

Due to excellent mechanical strength and corrosion resistance, stainless steel 316/316L is most widely used in a large number of equipment, tools, and machine parts in marine industry<sup>1,2,3</sup>. The marine components face the typical problem of heavy erosion in underwater conditions, leading to a drastic decrease in the efficiency of component which leads to huge economical loss. Therefore, the erosion wear in marine environment is still very serious concern for researchers. The erosion wear mainly arises due to the continuous impingement of silt particles that come with the water. In order to overcome such issue, the surface of steel is coated with various amorphous metallic coatings under the concept of surface engineering<sup>4,5</sup>. Surface engineering not only improves the aesthetic look and mechanical properties of substrate materials but also increases efficiency and service life at low cost. In this regard, coating technology is one of the major surface engineering techniques. The coating of metal and alloys, ferrous or non-ferrous, ceramics, etc., is deposited over base or substrate materials<sup>6,7</sup>. In various studies on Fe alloy coating materials, Fe-Cr-Ti alloy HVOF coating can provide unique properties such as low porosity, better mechanical, chemical, and magnetic and corrosion properties<sup>8,9,10</sup>. It was reported that by varying elemental

powder content, shape and size, porosity and pore size can be controlled, mechanical and corrosion resistance can be improved<sup>11</sup>. Sharma et al.<sup>12</sup> reviewed the significance of various factors on the performance of Fe coating materials. Fe alloy based amorphous metallic coating provides better mechanical properties like hardness, stress, wear resistance and better corrosion Zhou et al.<sup>13</sup>. Sharma et al.<sup>4</sup> further added that in coating technology, thermal spray coating such as HVOF coating leads to better coating quality, stronger cohesion and adhesion bond, better compaction and low porosity. In many industrial applications, where the surface properties like hardness, wear resistance and corrosion resistance are required to be improved, HVOF seems quite promising. HVOF coated Fe alloy based materials work efficiently in severe corrosive and abrasive environments. Xu et al.<sup>15</sup> stated that presence of WC-CoCr based composite coating reinforced with Fe alloy (35 wt.-%) prepared by HVOF coating techniques indicated better thermal stability and corrosion resistance as compared to WC-CoCr composite coating without Fe alloy. Apart from presence of Fe, chromium plays very important role to enhance corrosion and mechanical properties. In this regard, Chu et al.<sup>16</sup> deposited an amorphous Fe-Cr-Ti alloy HVOF coating Fe<sub>45</sub>Cr<sub>16</sub>Mo<sub>18</sub>C<sub>18</sub>B<sub>5</sub> on 316 stainless steel and observed an enhancement in corrosion

resistance. The HVOF coating process settings, however, have an impact on the coating materials' hardness<sup>17)</sup>. Kim et al.<sup>18)</sup> found that HVOF process atomized FeCrB surface protective coating on steel substrates to produce better mechanical properties, magnetic properties, low cost, better corrosion and wear resistance. The corrosion characteristics of iron alloy were studied by Bakare et al.<sup>19)</sup>, who came to the conclusion that the corrosion resistance in both 0.5M H<sub>2</sub>SO<sub>4</sub> and 3.5% NaCl would be higher for the higher degree of amorphous structure of the Fe-Cr-Ti alloy HVOF coating Fe<sub>43</sub>Cr<sub>16</sub>Mo<sub>16</sub>C<sub>15</sub>B<sub>10</sub>. The corrosion confrontation of iron alloys, like stainless steel, is enriched by chromium, as demonstrated by Suryanarayan and Inoue<sup>20)</sup>. Conversely, research reports that amorphous alloys based on Fe-Cr also show significant wear resistance<sup>21)</sup>. Compact strength was also shown to be increased by increasing the titanium content in the HVOF coating CrFeNiTi<sub>x</sub> (x = 0.2, 0.3, 0.4, 0.5, and 0.6 molar ratio) by Gao et al.<sup>22)</sup>. Furthermore, Liu et al.<sup>23)</sup> demonstrated that the mechanical characteristics and wear rate of coating materials were enhanced by the elemental composition. As a result, several variables, including as the ingredient proportion, heat treatment technique, and HOF coating parameters, affect the properties of coating materials. In case of a series of coating with varying chromium and titanium content, heat treated and untreated, one formulation of coating can be best in one property and another formulation of coating can be best on another property. Consequently, the best optimal coating should be determined using multi-criteria decision making (MCDM) taking into account all necessary and tested features<sup>24,25)</sup>. Material, GRA (Grey Relational approach), VIKOR (Vise Kriterijumska Optimizacija Kompromisno Resenje), and PSI (Preference Selection Index), TOPSIS and Analytical Hierarchy Process (AHP) have been used to find the best solution among a number of available solutions<sup>26,27,28)</sup>. However, Rahim et al.<sup>29)</sup> suggested fuzzy based TOPSIS as more effective tool in multi-criteria decision-making technique due to simplicity in use. They developed advanced materials by using MCDM technique under the constraint of safety, risk and environment risk. In order to better manage ambiguity and uncertainty in decision-making, fuzzy AHP (FAHP) expands on the conventional AHP approach by integrating fuzzy set theory. FAHP employs language variables and fuzzy numbers to describe subjective judgments in a more sophisticated manner than AHP, which depends on exact numerical comparisons. Because of this, FAHP is especially helpful when decision-makers are faced with vague or unclear information. Therefore, the aim of research was to find the possible solution for poor physical, mechanical properties, erosion wear and corrosion in steel-based component in marine environment. TOPSIS method was used to rank a series of Fe-Cr-Ti alloy HVOF coating materials with varying weight percentages of Cr and Ti on the basis of mechanical,

**Table 1:** Development of a covering material based on Fe alloys

Sample Designation		Fe (wt %)	Mo (wt %)	C (wt %)	Si (wt %)	Cr (wt %)	Ti (wt %)
FeMoCSi	C1	70	5	15	10	0	0
FeMoCSiCr 10	C2	60	5	15	10	10	0
FeMoCSiCr 20	C3	50	5	15	10	20	0
FeMoCSiTi 10	C4	60	5	15	10	0	10
FeMoCSiTi 20	C5	50	5	15	10	0	20
FeMoCSiCr 10 Ti10	C6	50	5	15	10	10	10

corrosion and wear properties.

## 2. Materials and methods

### 2.1. Materials and the deposition of coatings

All the materials constituents (Iron, Titanium, Chromium, Molybdenum, Silicon and Carbon) were purchased in the form of powder with the size range 50 to 90 μm from Jaipur (Mittal Materials). The mixture of powder with compositions as presented in Table 1 was kept in the graphite crucible and smelted in a gas metal atomizer (Indotherm gas atomizer, Jaipur, India) based on high pressure nitrogen gas atomization method at temperature up to 1700 K for a period of time until the composition of the metal liquids becomes homogeneous<sup>30,31,32)</sup>. Finally, the molten metal was ejected through nozzle and sieved in the size range of 100 to 150 μm. The SS-316L used as a substrate in the plate form that was delivered by Narendra Metal, Mumbai, India. 400 μm coating thickness was achieved by spraying the coating powder components (C1–C6) onto a stainless steel plate substrate of 110 mm × 110 mm × 3 mm. This was done using a HVOF thermal sprayer (Hippojet 2700, M/s Metallizing Equipment Co. Pvt. Ltd, Jodhpur, India). The coating process parameters used for coating deposition were oxygen flow rate of 250 slpm, LPG flow rate of 60slpm, oxygen pressure of 10 Kg/cm<sup>2</sup>, LPG Pressure of 6.5 kg/cm<sup>2</sup>, spray distance of 180 mm<sup>33,34,35)</sup>.

### 2.2. Solid Particle Erosion Wear Testing

Air jet erosion tester, Ducom, India was used to conduct erosion wear testing in accordance with ASTM G-76-13 test standard. Bangalore, India. Alumina abrasive particles was used as erodent. Every sample carefully weighted before test and after test. The change in weight of the sample was divided by the period of time to determine the

erosion wear rate. Wear properties were evaluated under two major wear parameters such as impingement angle and impact speed. Impingement angle and impact speed were kept at 30°, 90° and 35m/sec, 105m/sec respectively.

**2.3. Novel optimization techniques combining FAHP and TOPSIS**

A variety of MCDM techniques are applied to identify the best option from the list of options. This article uses a new FAHP and TOPSIS combo. The schematic diagram is shown in Figure 1. The weights of the several criteria were determined using the FAHP, and the TOPSIS approach was then used to obtain the best answer. Figure 1 shows that the complete optimization methodology consisted of two stages.

**Stage 1. FAHP Process**

Several performance determining attributes (PDAs) are found and categorised into two groups in the first stage and presented in Table 2.

Lower-the-better criteria (Porosity, Corrosion rate, Erosion wear rate at sliding speed of 35m/sec, 105 m/sec, at an impingement angle of 30° and 90°),

Higher-the-better criteria (Hardness, Adhesion Pull off strength, Fracture toughness)

Weightage is evaluated in two steps:

Step 1: A matrix of n×n was formed using the following equations, which are designated as Eqs. (1) and (2). Fuzzy numbers were allocated to each criterion using triangular fuzzy numbers (Table 3).

$$c_{ij} = 1, c_{ji} = \frac{1}{c_{ij}}, c_{ij} \neq 0 \tag{1}$$

$$C = \begin{bmatrix} c_{11} & \dots & c_{1n} \\ \vdots & \ddots & \vdots \\ c_{n1} & \dots & c_{nn} \end{bmatrix}, \tag{2}$$

Step 2: The fuzzy weights for each attribute in the pairwise comparison matrix are determined using the geometric mean technique. Equation (3) is utilised to compute the fuzzy geometric mean and fuzzy weights for every criteria.

$$r_i = [c_{i1} \times c_{i2} \times c_{i3} \dots \dots \times c_{in}]^{1/n} \tag{3}$$

Next, apply Eq. (4) to get the fuzzy weight of the i<sup>th</sup> attribute represented by a triangular fuzzy number.

$$W_i = r_i \times [r_1 + r_2 + \dots \dots + r_n]^{-1} \tag{4}$$

The weight for each criterion was determined by taking the mean of the triangle fuzzy number, which was then utilised for additional TOPSIS optimisation.

**Phase 2. TOPSIS procedure**

According to Eq. (5), a m×n performance matrix was built, where m is the number of potential solutions, n is the number of potential solutions, and n is the performance

defining attributes.

**Table 2:** Performance defining attributes for the comparative assessment

PDAs	Feature	Unit and Performance implications	Basic of selecting PDAs
PDA-1	Porosity	% Lower-the-better	It defines the percentage of voids, pores or air pockets within the coating material.
PDA-2	Corrosion rate	mm/year Lower-the-better	It defines the speed at which the coating material deteriorates due to chemical or electrochemical reaction.
PDA-3	Hardness	HV Higher-the-better	It defines coating material resistance against penetration
PDA-4	Adhesion Pull off strength	MPa Higher-the-better	It defines the force required to detach a coating from its substrate when a tensile force is applied perpendicular to the surface.
PDA-5	Fracture toughness	MPa.m <sup>1/2</sup> Higher-the-better	It defines the material's ability to resist the propagation of cracks when a flaw or crack is already present
PDA-6	Wear rate at sliding speed of 35m/sec	gm/min	It defines the wear rate of coating material when sliding speed was 35 m/sec
PDA-7	Wear rate at sliding speed of 105m/sec	gm/min Lower-the-better	It defines the wear rate of coating material when sliding speed was 105 m/sec
PDA-8	Wear rate at an impingement angle of 30°	gm/min Lower-the-better	It defines the wear rate of coating material when impingement angle was 30°.

PDA-9	Wear rate at an impingement angle of 90°	gm/min Lower-the-better	It defines the wear rate of coating material when impingement angle was 90°.
-------	--	----------------------------	--

**Table 3:** Fuzzy relational scale for comparing two objects in pairs

Absolute scale	Definition	Scale of Triangular Fuzzy numbers
1	Equally important	(1,1,1)
2	Weak importance	(1,2,3)
3	Moderate important	(2,3,4)
4	Moderately to strongly	(3,4,5)
5	strongly important	(4,5,6)
6	Fairly good important	(5,6,7)
7	Very strong important	(6,7,8)
8	Absolute	(7,8,9)
9	Extremely important	(8,9,10)

$$P_{M \times N} = \begin{matrix} A_1 \\ A_2 \\ \vdots \\ A_M \end{matrix} \begin{bmatrix} C_1 & C_2 & \dots & C_N \\ P_{11} & P_{12} & \dots & P_{1N} \\ P_{21} & P_{22} & \dots & P_{2N} \\ \vdots & \vdots & \ddots & \vdots \\ P_{M1} & P_{M2} & \dots & P_{MN} \end{bmatrix} \quad (5)$$

M alternatives and N PDAs are represented by Ai and Cj. Normalized matrix was constructed using Eq. (6)

$$\bar{X}_{ij} = \frac{x_{ij}}{\sqrt{\sum_{i=1}^n x_{ij}^2}} \quad (6)$$

Eq. (7) was used to form weighted normalized matrix by applying weightage derived from AHP.

$$V_{ij} = \bar{X}_{ij} \times W_j \quad (7)$$

Ideal best and ideal worst value were calculated. Euclidean distance was calculated from the ideal best and ideal worst using Eq. (8) and Eq. (9) respectively.

$$S_i^+ = \left[ \sum_{j=1}^m (V_{ij} - V_j^+)^2 \right]^{0.5} \quad (8)$$

$$S_i^- = \left[ \sum_{j=1}^m (V_{ij} - V_j^-)^2 \right]^{0.5} \quad (9)$$

Eq. (10) was used to calculate TPOSIS performance score.

$$TPSi = \frac{S_i^-}{S_i^- + S_i^+} \quad (10)$$

Fe-Cr-Ti alloy HVOF coating materials were ranked according to their optimal alloy composition using the TOPSIS score (TPSi) value. First on the list would be the solution with the greatest TOPSIS score, and last on the list

would be the answer with the lowest TOPSIS score.

### 3. Result and Discussion

#### 3.1. Impact of Cr and Ti alloying elements on wear rate at different impingement angles and impact speeds:

The effect of Cr and Ti as alloying element on wear rate of coating at varying speed (35m/sec and 105m/sec) under constant impingement angle of 60° was shown in Figure 2, Figure 3 illustrates the effects of Cr and Ti as alloying elements on coating wear rate at different impingement angles (30° and 90°) and constant impact speed (70 m/sec). In both the cases of Figure 2 and Figure 3, general trend of wear rate versus impact speed was seen. Wear rate increased with the impact speed. The major factor influencing the wear rate of iron, chromium and titanium based alloy is its micro-hardness of coating surface. Therefore, the materials with more hardness results in less wear<sup>36,37,38</sup>. Therefore, addition of chromium and titanium improved the wear resistance of coating materials. More hardness of titanium as compared to chromium was also

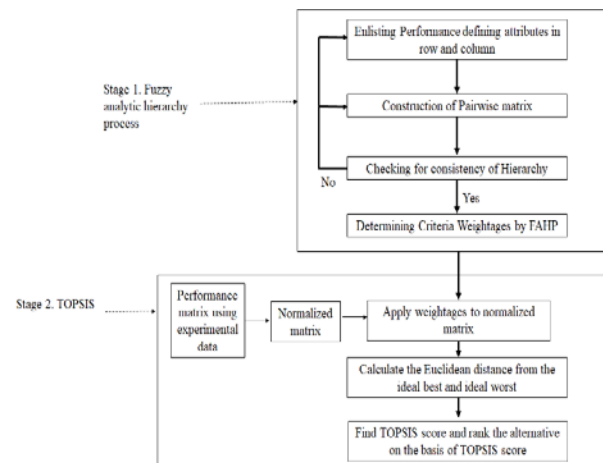


**Fig. 1:** Fuzzy analytic hierarchy + TOPSIS methodology

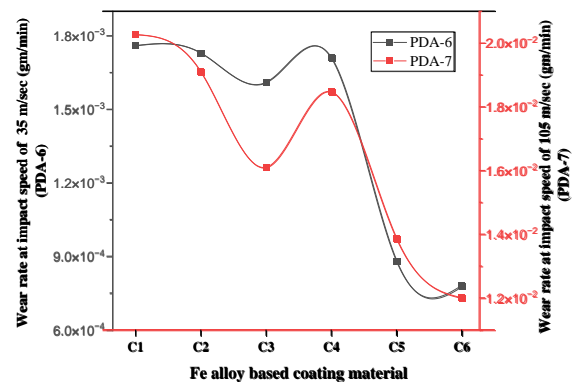


**Fig. 2** Wear rate of Fe-Cr-Ti alloy HVOF coating materials at 35m/sec and 105 m/sec impact speed: effects of chromium and titanium content

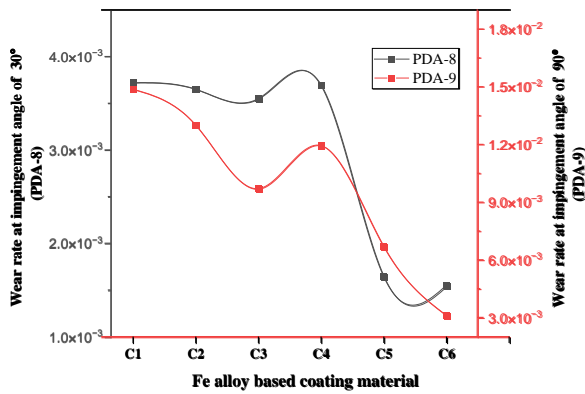


**Fig. 3:** Wear rate of Fe-Cr-Ti alloy HVOF coating materials at 30° and 90° impingement angles: effects of chromium and titanium content

reflection on wear performance. However, increase in wear rate despite of good hardness was due to decrease in fracture toughness. During the erosion wear process, fracture toughness has a greater impact on wear rate than hardness, which is more important during the abrasion wear process<sup>39,40,41</sup>. The wear rate was reduced by both titanium and chromium content when impact speed increased from 35 m/sec to 105 m/sec. Conversely, there was a modest drop in wear rate as the impingement angle varied, particularly at 90°, since there was no ploughing phenomenon.

### 3.2. Ranking of the Fe-Cr-Ti alloy HVOF coating materials

Chromium and titanium added Fe-Cr-Ti alloy HVOF coating were finally optimized to find the best coating using a novel MCDM techniques which was combination of FAHP and TOPSIS. The geometric mean of weightage of triangular fuzzy number was presented in Table 4. Table 4 also shows the final weightage for each criteria which was calculated by taking mean of three TFN. Final

**Table 4:** Comparison matrix results with FAHP

PDAs	Fuzzy Weight criteria	Mean weightage
PDA-1	0.167, 0.146, 0.502	0.167
PDA-2	0.052, 0.049, 0.158	0.053
PDA-3	0.256, 0.259, 0.747	0.249
PDA-4	0.176, 0.192, 0.526	0.175
PDA-5	0.155, 0.173, 0.473	0.158
PDA-6	0.049, 0.045, 0.149	0.050
PDA-7	0.049, 0.045, 0.149	0.050
PDA-8	0.049, 0.045, 0.149	0.050
PDA-9	0.049, 0.045, 0.149	0.050

**Table 5:** Experimental data of performance defining attributes

Coatings	C1	C2	C3	C4	C5	C6
PDA-1	0.9	1.0	1.0	1.3	1.3	1.4
PDA-2	4.1	3.2	2.1	3.9	3.0	2.1
PDA-3	405	495	710	645	800	870
PDA-4	18.0	22.0	26.9	19.2	22.6	28.8
PDA-5	1.2	1.4	2.1	1.8	2.3	2.5
PDA-6	0.002	0.002	0.002	0.002	0.001	0.001
PDA-7	0.020	0.019	0.016	0.018	0.014	0.012
PDA-8	0.004	0.004	0.004	0.004	0.002	0.002
PDA-9	0.015	0.013	0.010	0.012	0.007	0.003

**Table 6:** Normalized matrix

Coating	C1	C2	C3	C4	C5	C6
PDA-1	0.31	0.34	0.37	0.44	0.46	0.49
PDA-2	0.52	0.41	0.27	0.51	0.39	0.27
PDA-3	0.25	0.3	0.43	0.39	0.48	0.53
PDA-4	0.32	0.39	0.47	0.34	0.4	0.51
PDA-5	0.25	0.29	0.44	0.38	0.49	0.53
PDA-6	0.49	0.48	0.45	0.47	0.24	0.22
PDA-7	0.49	0.46	0.39	0.45	0.33	0.29
PDA-8	0.49	0.48	0.46	0.48	0.21	0.2
PDA-9	0.57	0.5	0.37	0.46	0.26	0.12

optimization was done using TOPSIS method. The experimental data of performance defining attributes was presented in Table 5. Normalized data was obtained using Eq. (6) and presented in Table 6. The weightage obtained for each criteria using AHP was supplied to normalized data (Eq. (7)) to obtained weighted normalized matrix and presented in Table 7. Euclidean distance was calculated from the ideal best and ideal worst using Eq. (8) and Eq. (9) respectively and used to calculate final TOPSIS score and presented in Table 8. On the basis of TOPSIS score, the rank of each coating is depicted in Figure 4. Figure 4 clearly shows that the ranking of Fe-Cr-Ti alloy HVOF coating was in the order from the best to the lowest as C6, C5, C4, C3, C2, and C1. It can be observed that the TOPSIS score of C6 was highest (0.748) and hence C6 indicated as the most important coating among the available choices.

**Table 7:** Weighted Normalized matrix

Coatings	C1	C2	C3	C4	C5	C6	V+ (Ideal Best)	V- (Ideal Worst)
PDA-1	0.051	0.057	0.061	0.074	0.077	0.083	0.051	0.083
PDA-2	0.028	0.022	0.015	0.027	0.021	0.014	0.014	0.028
PDA-3	0.061	0.075	0.07	0.097	0.021	0.031	0.031	0.061
PDA-4	0.055	0.068	0.083	0.059	0.069	0.089	0.089	0.055
PDA-5	0.04	0.046	0.07	0.06	0.077	0.083	0.083	0.04
PDA-6	0.024	0.024	0.022	0.024	0.012	0.011	0.012	0.024
PDA-7	0.024	0.023	0.019	0.022	0.017	0.015	0.017	0.024
PDA-8	0.024	0.024	0.023	0.024	0.011	0.01	0.011	0.024
PDA-9	0.028	0.025	0.019	0.023	0.013	0.006	0.013	0.028

**Table 8:** TOPSIS Score performance matrix

Coating	Si+ (Euclidean distance from the ideal best)	Si- (Euclidean distance from the ideal worst)	Pi (TOPSIS Performance Score)
C1	0.093	0.031	0.251
C2	0.075	0.033	0.306
C3	0.035	0.067	0.66
C4	0.061	0.043	0.414
C5	0.035	0.076	0.685
C6	0.032	0.095	0.748

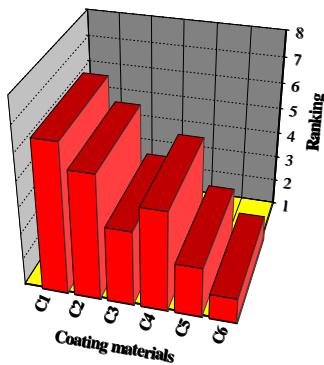


**Fig. 4:** Ranking of the Fe alloy based coating materials

### 4. Conclusion

The current study addressed a major issue of machine component utilised in the maritime industry. Heavy slurry erosion reduces the efficiency and longevity of steel components, resulting in significant financial loss and an influence on safety. A comprehensive evaluation of the mechanical and wear characteristics of six distinct compositions of iron, chromium, and titanium based alloy HVOF coated materials with varying titanium and chromium concentration was conducted on 316L steel. In terms of mechanical and wear qualities, there were nine criteria: erosion wear rate at different impingement angles and impact speeds, hardness, porosity, adhesion strength, corrosion rate, and fracture toughness. When it comes to hardness, adhesion pull off strength, corrosion rate, and wear rate, titanium appears to be more important than chromium. Nonetheless, chromium was more significant than titanium in terms of porosity and resistance to corrosion. Ultimately, the optimal performance in terms of mechanical characteristics and corrosion was suggested by the combination of both alloying components. As a result, HVOF coating with titanium and chromium (C6) proved to be the most popular coating material.

### Declaration of interests

The authors state that they have no known competing financial interests, either direct or indirect, related to this investigation.

### Data availability statement

Since the raw or processed data are currently being utilised in an ongoing research, we are unable to provide them now in order to duplicate these results.

### References

- 1) H.-B. Lee, T.-J. Lin, C.-Y. Lee, "Corrosion of high-velocity-oxygen-fuel (HVOF) sprayed non-crystalline alloy coating in marine environment." *Surface and Coatings Technology* 409 (2021) 126896. <https://doi.org/10.1016/j.surfcoat.2021.126896>.
- 2) M. Cherigui, H.I. Feraoun, N.E. Feninehe, H. "Structure of amorphous iron-based coatings processed by HVOF and APS thermally spraying." *Materials Chemistry and Physics* 85.1 (2004): 113-119. <https://doi.org/10.1016/j.matchemphys.2003.12.017>.
- 3) S. Kumar, Akash, Anil K C, Kumaraswamy, Solid particle erosion performance of multi-layered carbide coatings (WC-SiC-Cr<sub>3</sub>C<sub>2</sub>), *Evergreen* 10 (2023) 813–819. <https://doi.org/10.5109/6792833>.
- 4) Y. Mohd-Azmi, F. Ahmad, S. Kabir, N. Nosbi, Y.G.

- Heng, A. Zulfiqar, Analysis of thermal performance of mica-mineral reinforced intumescent coating for structural steel application, *Evergreen* 8 (2021) 565–573. <https://doi.org/10.5109/4491648>.
- 5) V. Dubey, K. Pandey, H. Kumar, P.K. Arora, J.K. Katiyar, A.K. Sharma, Tribological behaviour of AISI 304 steel on electrodeposited hard chrome coated steel, *Evergreen* 11 (2024) 1210–1215. <https://doi.org/10.5109/7183426>.
  - 6) D. Chandra, N.R. Chauhan, Effect of ceramic coating on mechanical properties of AZ31 magnesium alloy, *Evergreen* 11 (2024) 1732–1739. <https://doi.org/10.5109/7236825>.
  - 7) V. Hutsaylyuk, M. Student, K. Zadorozhna, O. Student, H. Veselivska, V. Gvosdetskii, P. Maruschak, H. "Improvement of wear resistance of aluminum alloy by HVOF method." *Journal of Materials Research and Technology* 9.6 (2020): 16367-16377. <https://doi.org/10.1016/j.jmrt.2020.11.102>.
  - 8) R.K. Sharma, R.K. Das, S.R. Kumar, Effect of HVOF spraying parameters on fracture, erosion and thermal properties of Fe alloy-based coating materials. *Proc Inst Mech Eng L J Mater Des Appl* 235(2021)1703–11. <https://doi.org/10.1177/1464420721999682>.
  - 9) R.K. Sharma, R.K. Das, S.R. Kumar, "Microstructure, mechanical and tribological properties of high velocity oxy fuel thermal spray coating: A review," *Materwiss Werksttech* 54(2023)90–7. <https://doi.org/10.1002/mawe.202200101>.
  - 10) R.K. Sharma, R.K. Das, S.R. Kumar, "Microstructure, mechanical and erosion wear analysis of Post Heat treated Fe alloy based coating with varying chromium," *Materwiss Werksttech*. 52(2021) 1173–1184. <https://doi.org/10.1002/mawe.202100080>.
  - 11) Xu W, Lu X, Zhang B, Liu C, Lv S, Yang S, et al. "Effects of porosity on mechanical properties and corrosion resistances of PM-fabricated porous Ti-10Mo alloy." *Metals* 8.3 (2018) 188. <https://doi.org/10.3390/met8030188>.
  - 12) R.K. Sharma, R.K. Das, S.R. Kumar, "Microstructure, adhesion and erosion properties of Fe-Cr-Ti-Mo-C-Si coating with varying Titanium," *Mater Today Commun* (2020) 101826. <https://doi.org/10.1016/j.mtcomm.2020.101826>.
  - 13) Z. Zhou, L. Wang, F.C. Wang, H.F. Zhang, Y.B. Liu, S.H. Xu, "Formation and corrosion behavior of Fe-based amorphous metallic coatings by HVOF thermal spraying," *Surface and Coatings Technology* 204.5 (2009) 563-570. <https://doi.org/10.1016/j.surfcoat.2009.08.025>
  - 14) R.K. Sharma, R.K. Das, S.R. Kumar, "Effect of chromium content on microstructure, mechanical and erosion properties of Fe-Cr-Ti-Mo-C-Si coating," *Surf Interf* 22(2021) 100820. <https://doi.org/10.1016/j.surfin.2020.100820>.
  - 15) L.P. Xu, J.B. Song, C.G. Deng, L. Mingyong, H. Zheng, "Microstructure and Properties of WC-based Coating Reinforced by Fe-based Amorphous Alloys." *RARE METAL MATERIALS AND ENGINEERING* 49.5 (2020) 1546-1552. <https://doi.org/10.12442/j.issn.1002-185X.20181278>
  - 16) Z. Chu, W. Deng, X. Zheng, Y. Zhou, C. Zhang, J. Xu, L. Gao, "Corrosion mechanism of plasma-sprayed fe-based amorphous coatings with high corrosion resistance." *Journal of Thermal Spray Technology* 29 (2020) 1111-1118. <https://doi.org/10.1007/s11666-020-01030-9>
  - 17) W. Fanga, T.W. Choa, J.H. Yoona, K.O. Song, S.K. Hur, S.J. Youn, H.G. Chun, "Processing optimization, surface properties and wear behavior of HVOF spraying WC–CrC–Ni coating." *Journal of materials processing technology* 209.7 (2009) 3561-3567. <https://doi.org/10.1016/j.jmatprotec.2008.08.024>
  - 18) H.J. Kim, S. Grossi, Y.G. Kweon, "Wear performance of metamorphic alloy coatings." *Wear* 232.1 (1999) 51-60. [https://doi.org/10.1016/S0043-1648\(99\)00160-X](https://doi.org/10.1016/S0043-1648(99)00160-X)
  - 19) M.S. Bakare, K.T. Voisey, K. Chokethawai, et al., "Corrosion behaviour of crystalline and amorphous forms of the glass forming alloy Fe43Cr16Mo16C15B10." *Journal of Alloys and Compounds* 527 (2012) 210-218. <https://doi.org/10.1016/j.jallcom.2012.02.127>
  - 20) C. Suryanarayana, A. Inoue, "Iron-based bulk metallic glasses." *International Materials Reviews* 58.3 (2013) 131-166. <https://doi.org/10.1179/1743280412Y.0000000007>
  - 21) R.K. Sharma, R.K. Das, S.R. Kumar, "Effect of chromium–titanium on corrosion and erosion of HVOF coating." *Surface Engineering* 38.4 (2022) 366-374. <https://doi.org/10.1080/02670844.2022.2076015>
  - 22) Gao S, Kong T, Zhang M, Chen X, Sui YW, Ren YJ, Qi JQ, Wei FX, He YZ, Meng QK, Sun Z. "Effects of titanium addition on microstructure and mechanical properties of CrFeNiTi<sub>x</sub> (x= 0.2–0.6) compositionally complex alloys." *Journal of Materials Research* 34.5 (2019) 819-828. DOI: <https://doi.org/10.1557/jmr.2019.40>
  - 23) Z. Liu, E. Liu, S. Du, C. Li, H. Du, Y. Bai, "Effect of Heat Treatment on Microstructure and Tribocorrosion Performance of Laser Cladding Ni -

- 65 WC Coating." *Scanning* 2020.1 (2020) 4843175. <https://doi.org/10.1155/2020/4843175>
- 24) Z. Zhu, L. Xu, G. Chen, L. Yilei, "Optimization on tribological properties of aramid fibre and CaSO<sub>4</sub> whisker reinforced non-metallic friction material with analytic hierarchy process and preference ranking organization method for enrichment evaluations." *Materials & Design* 31.1 (2010): 551-555. <https://doi.org/10.1016/j.matdes.2009.07.015>
  - 25) S.R. Kumar, A. Patnaik, I.K. Bhat, T.Singh, "Optimum selection of nano-and microsized filler for the best combination of physical, mechanical, and wear properties of dental composites." *Proceedings of the Institution of Mechanical Engineers, Part L: Journal of Materials: Design and Applications* 232.5 (2018) 416-428. <https://doi.org/10.1177/1464420716629825>
  - 26) S.R. Kumar, A. Patnaik, A. Sharma, S. Alam and C. Sharma, "Grey relational analysis of microcapsule- and nanoalumina-reinforced dental composite based on mechanical and wear performance." *Journal of Bio-and Tribo-Corrosion* 4 (2018): 1-10. <https://doi.org/10.1007/s40735-018-0175-7>.
  - 27) R. Verma, M.S. Azam, S.R. Kumar, "Performance evaluation of glass ionomer and alumina-silica nanoparticle reinforced dental composite using preference selection index." *Polymer Composites* 43.6 (2022) 3745-3752. <https://doi.org/10.1002/pc.26652>.
  - 28) J. Bhadu, J. Bhamu, P. Saraswat, An analytic hierarchy process (AHP) approach for prioritizing the industries 4.0 technologies (I4.0T), *Evergreen* 10 (2023) 667–675. <https://doi.org/10.5109/6792813>.
  - 29) A.A. Rahim, S.N. Musa, S. Ramesh, M.K. Lim, "Development of a fuzzy-TOPSIS multi-criteria decision-making model for material selection with the integration of safety, health and environment risk assessment." *Proceedings of the Institution of Mechanical Engineers, Part L: Journal of Materials: Design and Applications* 235.7 (2021) 1532-1550. <https://doi.org/10.1177/1464420721994269>.
  - 30) S.R. Kumar, R.K. Sharma, "Current insights into the factors affecting the erosion behaviour of iron alloy based coating material." *Materialwissenschaft und Werkstofftechnik* 55.1 (2024) 80-88. <https://doi.org/10.1002/mawe.202300062>.
  - 31) M. Pantoja, F. Velasco, J. Abenojar, M.A. Martinez, "Development of superhydrophobic coatings on AISI 304 austenitic stainless steel with different surface pretreatments." *Thin Solid Films* 671 (2019) 22-30. <https://doi.org/10.1016/j.tsf.2018.12.016>.
  - 32) C. Rodríguez-Villanueva, N. Encinas, J. Abenojar, M.A. Martínez, "Assessment of atmospheric plasma treatment cleaning effect on steel surfaces." *Surface and Coatings Technology* 236 (2013) 450-456. <https://doi.org/10.1016/j.surfcoat.2013.10.036>.
  - 33) Chau, Pan, Yang, "Preparation of gas-atomized Fe-based alloy powders and HVOF sprayed coatings" *Adv. Mater. Res.* 6 (2017) 343–348. <https://doi.org/10.12989/amr.2017.6.4.343>
  - 34) R.A. Mahesh, R. Jayaganthan, S. Prakash, "High temperature oxidation studies on HVOF sprayed NiCrAl coatings on superalloys." *Surface engineering* 27.5 (2011) 332-339. <https://doi.org/10.1179/174329409x409486>.
  - 35) S. Tailor, A. Modi, S.C. Modi, "High-performance molybdenum coating by wire-HVOF thermal spray process." *Journal of Thermal Spray Technology* 27.4 (2018) 757-768. <https://doi.org/10.1007/s11666-018-0706-2>.
  - 36) R.K. Sharma, R.K. Das, S.R. Kumar, "Effect of varying chromium and titanium content on corrosion, mechanical and solid particle erosion properties of iron alloy based coating." *Materialwissenschaft und Werkstofftechnik* 53.6 (2022) 675-685. <https://doi.org/10.1002/mawe.202100409>
  - 37) L. Qiao, Y. Wu, S. Hong, J. Cheng, Z. Wei, "Influence of the high-velocity oxygen-fuel spray parameters on the porosity and corrosion resistance of iron-based amorphous coatings." *Surface and Coatings Technology* 366 (2019) 296-302. <https://doi.org/10.1016/j.surfcoat.2019.03.046>
  - 38) C. Zeng, W. Tian, W.H. Liao, L. Hua, "Microstructure and porosity evaluation in laser-cladding deposited Ni-based coatings." *Surface and Coatings Technology* 294 (2016) 122-130. <https://doi.org/10.1016/j.surfcoat.2016.03.083>
  - 39) H. Luo, H. Su, C. Dong, et al. "Passivation and electrochemical behavior of 316L stainless steel in chlorinated simulated concrete pore solution." *Applied Surface Science* 400 (2017) 38-48. <https://doi.org/10.1016/j.apsusc.2016.12.180>.
  - 40) R.K. Sharma, R.K. Das, S.R. Kumar, "HVOF Deposition, comparative investigation and optimum selection of molybdenum, boron, chromium, and titanium in Iron amorphous composite coatings." *Surface Engineering* 39.4 (2023) 481-494. <https://doi.org/10.1080/02670844.2023.2233263>.
  - 41) R.K. Sharma, R.K. Das, S.R. Kumar, "Investigation of solid particle erosion behaviour of Fe-Cr alloy coating." *International Journal of Surface Science and Engineering* 17.1 (2023) 44-57. <https://doi.org/10.1504/IJSURFSE.2023.128886>